Arab J Sci Eng (2017) 42:1751–1764
DOI 10.1007/s13369-016-2295-z

RESEARCH ARTICLE - MECHANICAL ENGINEERING

Fabrication of NanoSiC-Reinforced Al2024 Matrix Composites by a Novel Production Method

Temel Varol[1] · **Aykut Canakci**[1] · **Emre Deniz Yalcin**[2]

Received: 1 March 2016 / Accepted: 17 August 2016 / Published online: 30 August 2016

Abstract In this paper, flake powder metallurgy technique is described for fabricating near-net-shape SiC nanoparticle-reinforced Al2024 matrix composites. The effect of the particle size on the flake Al2024 matrix powders and the amount of SiC nanoparticles in the particle distribution, microstructure, relative density, and hardness of SiC nanoparticle-reinforced Al2024 matrix composites were investigated. The flake Al2024 matrix powders were mixed with three different as-received Al2024 powders particle sizes by ball milling. Microstructural characterization revealed a flake-like microstructure and dispersed SiC nanoparticles between the Al2024 matrix powders with grain boundaries containing sufficient area for the reinforcement particles. The hot pressed density increased as the matrix size decreased due to the small frictional forces observed between the fine flake particles. The hardness of Al2024/SiC nanocomposites increased as the size of the Al2024 matrix powders decreased.

Keywords Metal–matrix composites · Ball milling · Nanocomposite · Flake powder metallurgy · SiC

1 Introduction

The need for advanced engineering materials is constantly increasing in the aerospace, transportation, defense, and energy industries because a single material generally cannot meet the requirements for numerous different applications [1,2]. El-Kady and Fathy [3] fabricated Al-SiC composites by using powder metallurgy method. They investigated the effect of SiC particle size and its amount on both physical and mechanical properties of Al matrix composite. Canakci and Varol [4] produced AA7075/Al-SiC composites from machining chips using powder metallurgy technique. They studied the effect of SiC content on the microstructure, physical and mechanical properties of AA7075/Al-SiC composites. There is growing interest in the automotive, aerospace, and transportation industries in aluminum matrix composites (AMCs) because of their light weight, high elastic modulus, improved strength, and good wear resistance [5]. 2024 aluminum alloys is widely used in aerospace applications due to their low density and good damage tolerance [6]. Kök [7] investigated abrasive wear of Al_2O_3 particle-reinforced 2024 aluminum alloy matrix composites. He reported that the wear resistance of the composites was considerably bigger than that of the aluminum alloy. SiC is an important reinforcement material for Al metal matrix composites because of its high strength and modulus of elasticity. The addition of nanometer-sized SiC further promotes increases to both the mechanical properties and ductility of composites [8].

Powder metallurgy (PM) is widely used as a fabrication method to produce metal matrix composites. Although PM allows the production of components with complex geometries in bulk, there are some disadvantages associated with conventional powder metallurgy, such as porosity and agglomeration of the reinforcing particles within the metal matrix. This often leads to the degradation of the bulk mechanical properties. These problems become more important when there is a significant difference in the particle sizes between the reinforcement and the matrix alloy powders or when the reinforcement volume fraction is high [9,10].

✉ Temel Varol
tvarol@ktu.edu.tr

[1] Department of Metallurgical and Materials Engineering Engineering Faculty, Karadeniz Technical University, Trabzon, Turkey

[2] Abdullah Kanca Vocational School of Higher Education, Karadeniz Technical University, Trabzon, Turkey

Umasankar et al. [11] studied the influence of processing parameters on the mechanical properties of SiC particle-reinforced AA6061 aluminum alloy matrix composite by powder metallurgy technique. They stated that when the content of SiC particle increases, localized agglomeration of the reinforcement was observed which resulting in certain heterogeneity of the microstructure. Mechanical milling is an attractive powder metallurgy technique that produces a uniform dispersion of the reinforcement particles within the matrix through a repeated process of cold welding, fracturing and rewelding, which gives rise to the reinforcement particles being well embedded in the matrix [12,13]. However, the high degree of work deformation reduces the ductility of matrix material, and the compressibility of the alloy and composite powders decreases as a result of the work hardening process. Therefore, it is essential to develop a simple way for uniform distribution of the reinforcement particles into the matrix, to ensure an adequate powder deformation capacity and promote good mechanical properties in the deformation-processed MMCs. Recently, a new and simple method known as "flake powder metallurgy" (FPM) has been developed for fabricating MMCs. In this method, the flake morphology of milled powders permits fabrication without requiring extended milling times and ensures a homogeneous distribution of the reinforcement particles in the matrix [14,15]. Zhang et al. [16] synthesized Al-Al_2O_3 composites by means of a flake powder metallurgy. They reported that both the decrease in grain size of Al matrix and the increase in volume fraction of Al_2O_3 contribute to the increase in tensile strength caused by decreasing flake Al powder thickness.

Although, the microstructure, physical and mechanical properties of metal matrix composites have been examined and reviewed in several works using micron-sized reinforcing materials and powder metallurgy methods [17,18], studies especially related to Al2024 matrix nanocomposites with reinforced nanosized reinforcement materials and flake powder metallurgy methods are limited. To address this shortcoming, we present a study on the production of Al2024/SiC nanocomposites with varying amounts of SiC particle reinforcement using a flake powder metallurgy fabrication technique. The effect of the weight percentage of SiC nanoparticles and the milling methods on the particle agglomeration and microstructure are examined. Finally, changes in the physical and mechanical properties as a function of SiC content were investigated using density, hardness, and tensile strength measurements.

2 Experimental Procedures

Al2024 matrix powder (Gündoğdu Exoterm Company, Turkey) with average particle sizes of 28, 62 and 162 μm were used as the matrix materials (Fig. 1). The chemical composition of the as atomized Al2024 alloy powders was given in Table 1. SiC powder with an average particle size of 40 nm was procured from Alfa Aesar (Fig. 2). The starting Al powders had an irregular morphology, whereas the SiC nanoparticles were polygonal or angular in shape.

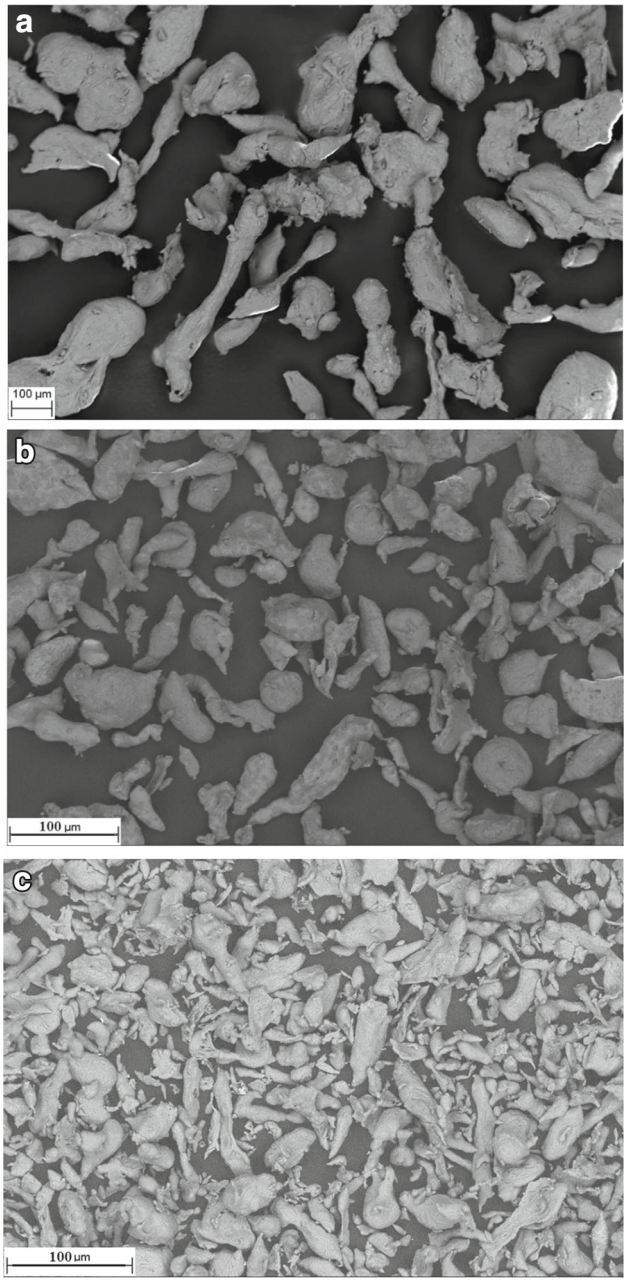

Fig. 1 SEM images of the starting matrix powders: Al2024 powder with **a** 162 μm particle size, **b** 60 μm particle size and **c** 28 μm particle size

The fabrication of the flake nanoSiC particle-reinforced Al2024 alloy composite powder was carried out in two stages. To produce the flake powder metallurgy Al2024 matrix powder, a milling process was performed at room temperature using tungsten carbide balls in a planetary ball mill (Retsch

Table 1 Chemical composition of Al2024 alloy

	Cu	Mg	Mn	Fe	Si	Cr	Zn	Ti	Al
wt%	4.85	1.78	0.312	0.374	0.385	0.042	0.138	0.005	92.114

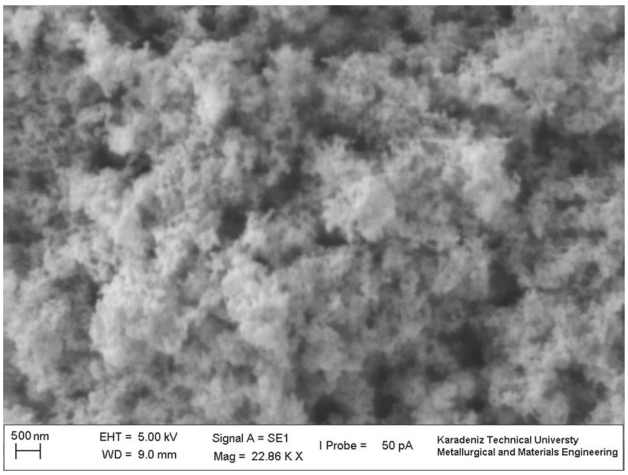

Fig. 2 SEM image of the SiC nanoparticles

PM 200). The ball-to-powder weight ratio and rotational speed were 10:1 and 300 rpm, respectively. Methanol (1 wt%) was used as the process control agent (PCA) to prevent excessive cold welding of powder particles. The main goal of the first stage was to determine the most suitable flake morphologies for use in manufacturing the composite samples. Five different milling times (0.5, 1, 1.5, 2, and 5 h) were selected during the first stage. The ball mills were 10 mm in diameter, and the weight ratio of ball to powder (BPR) was maintained at 10:1. To fabricate the flake powder metallurgy Al2024/SiC nanocomposite powder, various nominal portions of 1, 3, and 5 wt% SiC nanopowder were added to the atomized Al matrix powders. The Al2024 alloy matrix powders and nanoSiC reinforcement particles were milled together for 15 min in the second stage. The purpose of the second stage was to embed the SiC nanoparticles in the matrix powder.

The apparent density of the composite powders was measured using a Standard Hall Flowmeter. The morphology of the initial powders, flake powders, distribution of the SiC nanoparticles within the Al2024 matrix and the microstructure of nanoSiC particle-reinforced Al2024 matrix composites were examined using a scanning electron microscope (SEM) (Zeiss Evo LS10). X-ray mapping was also performed on the milled powders to evaluate the elemental distribution. A Mastersizer Hydro 2000e laser particle size analyzer was utilized to determine both the average particle size and size distribution of the produced powders. The Al2024/SiC nanocomposite powders were consolidated via hot pressing (HP) using a steel die with a diameter of 30 mm, a load of 150 MPa, a temperature of 500°C, and a soaking

Table 2 Theoretical density of AL2024-SiC nanocomposites

Composite			
	Al2024-1 wt%SiC	Al2024-3 wt%SiC	Al2024-5 wt%SiC
Theoretical density (g/cm^3)	2.8041	2.8123	2.8205

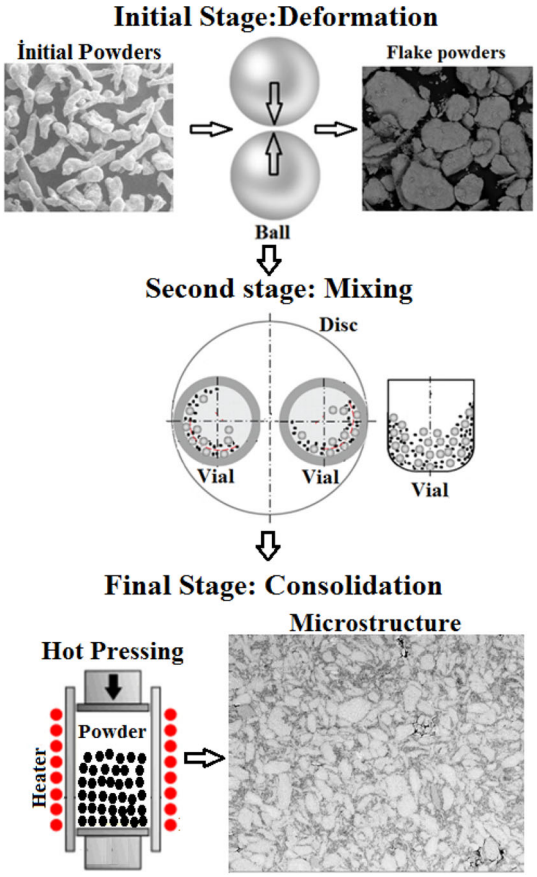

Fig. 3 The different stages of the flake powder metallurgy process

time of 45 min. The density (d) of the compacted material was determined by Archimedes' method. The theoretical density of the compacted material was calculated from the rule of mixtures using the densities of Al2024 (2.8 g/cm^3) and nanoSiC (3.21 g/cm^3) particles (Table 2). The hardness measurements were performed by using a Brinell hardness tester (INNOVATEST, NEMESIS 9000) with a load of 31.25 kgf. The hardness values were averaged over four measurements taken at different places on the sample.

3 Results and Discussion

3.1 The Change of Flake Morphology

The first and most important step in the flake powder metallurgy method is the deformation process. During defor-

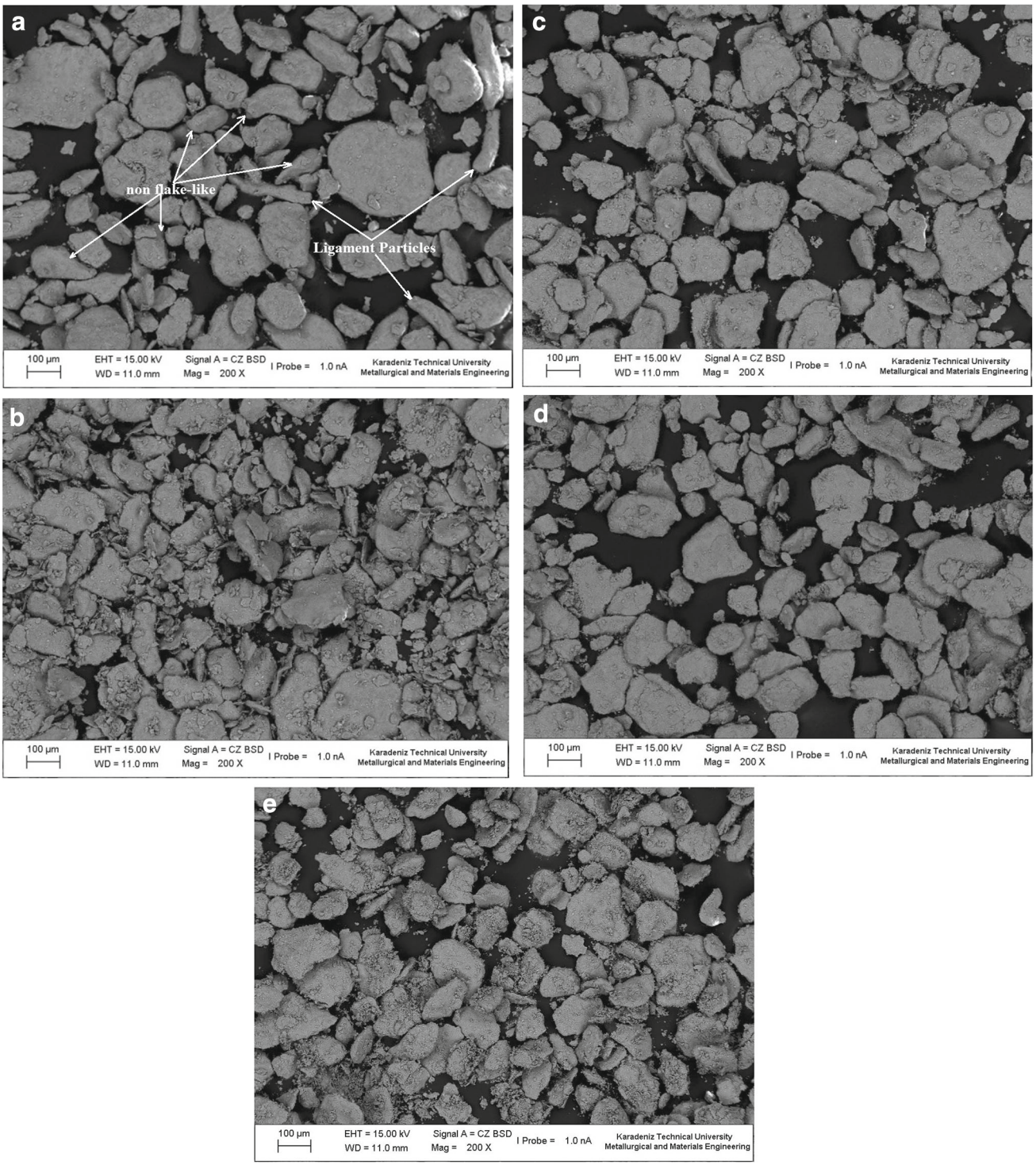

Fig. 4 The morphology CMS matrix powders as a function of milling time: **a** 0.5 h, **b** 1 h, **c** 1.5 h, **d** 2 h and **e** 2.5 h

mation, the initial morphology of the as-received powders is changed to flake morphology through the ball–powder–ball collisions (Fig. 3) [19]. However, the morphological conversion from the initial morphology (irregular or spherical) to flake morphology may be explained using a time period rather than a definite milling time. This is because the powder is gradually exposed to plastic deformation during the ball milling process. The initial stage in the flake powder metallurgy method has the same characteristics as the first stage of a ductile-ductile milling system [20]. The

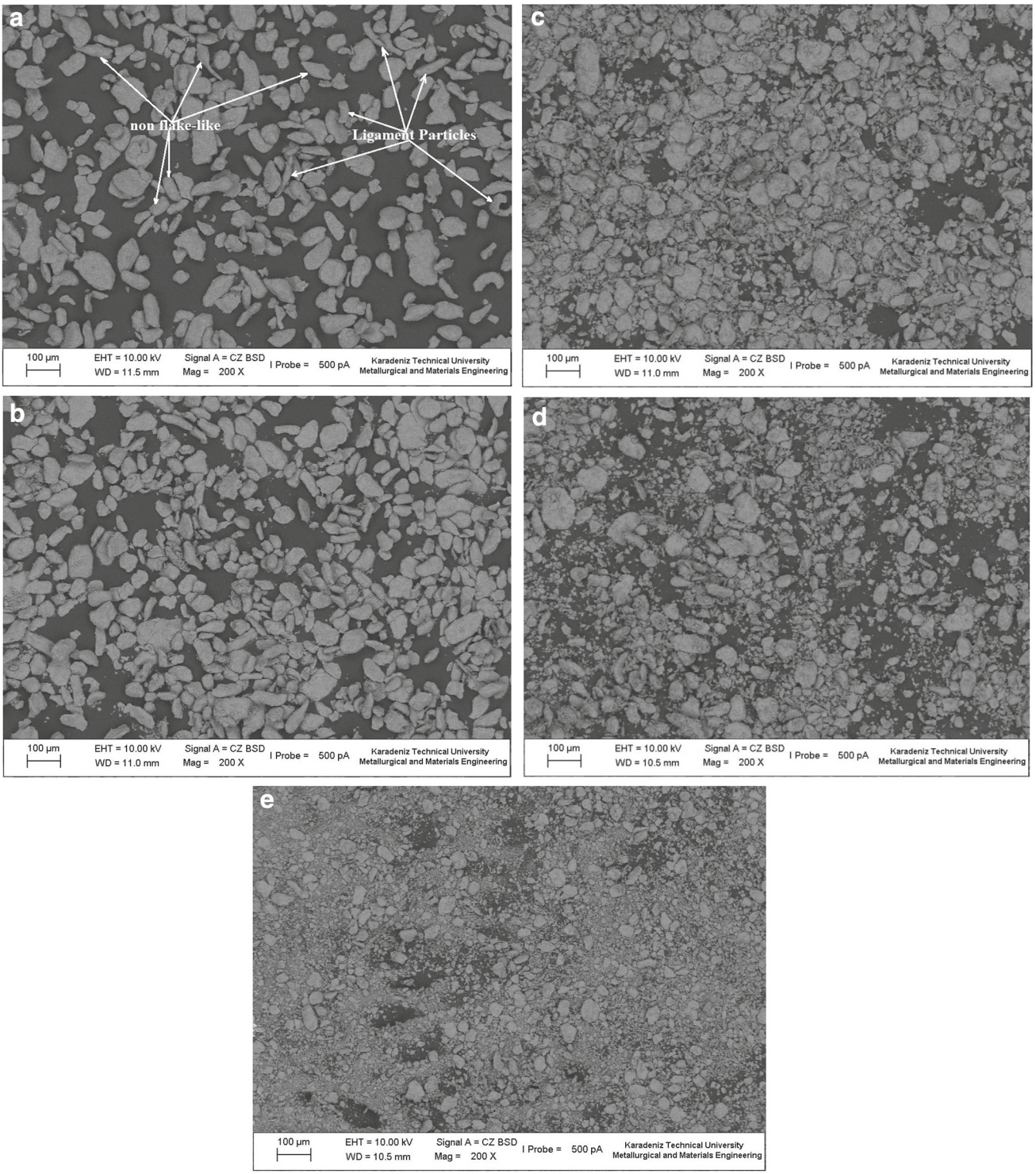

Fig. 5 The morphology of MMS matrix powders as a function of milling time: **a** 0.5 h, **b** 1 h, **c** 1.5 h, **d** 2 h and **e** 2.5 h

main difference is that the metal powder mass has the same chemical composition that is used in flake powder metallurgy, whereas in a ductile–ductile system, the two metal powder masses have different chemical compositions. The second stage in the flake powder metallurgy method is mixing the flake matrix powders and ceramic particles. This process may be performed using a simple mechanical stirrer, but a more homogeneous mixture can be obtained using the ball milling technique. It is noted that deformation effects, fracturing and cold welding should not occur during the mixing process.

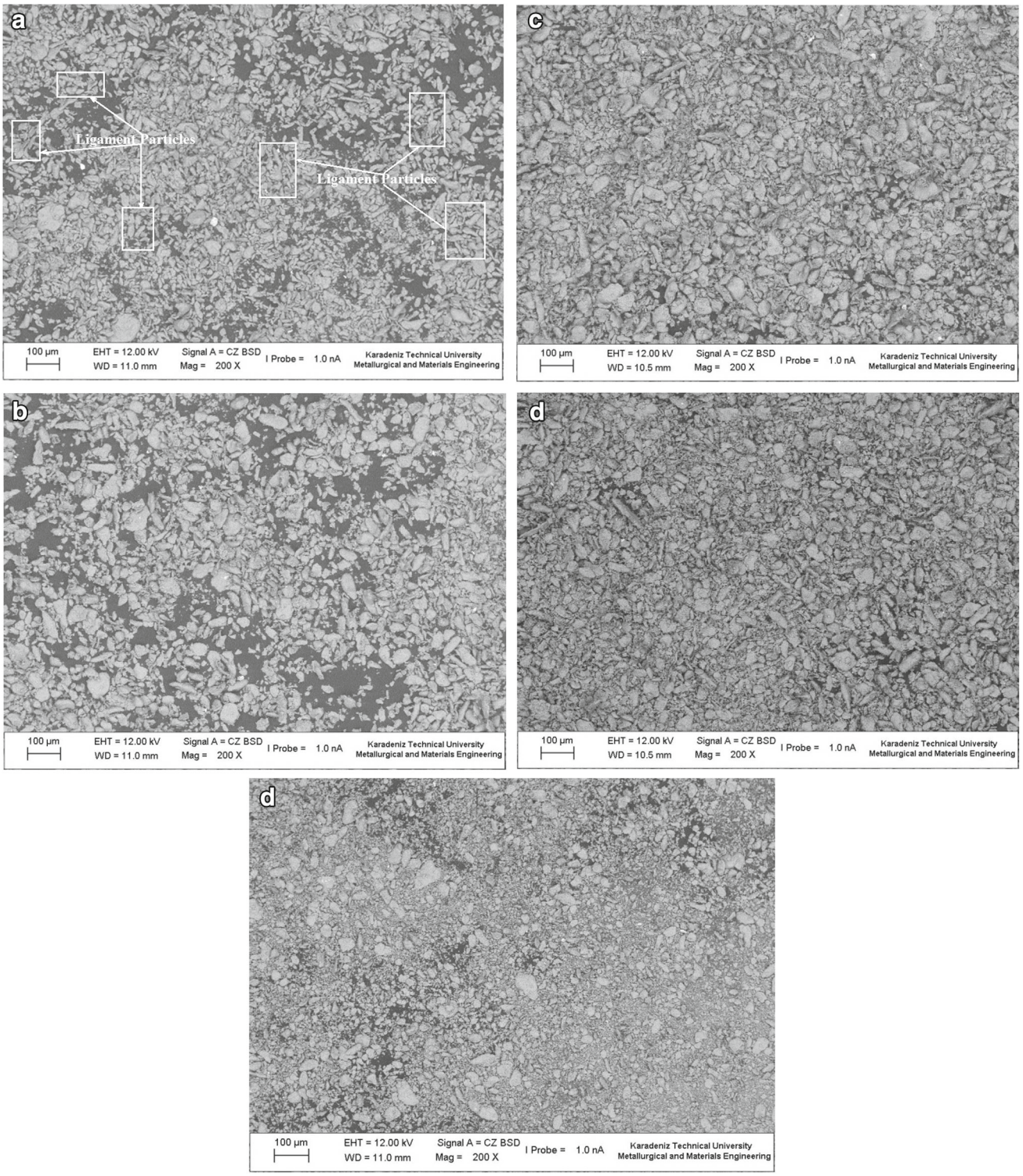

Fig. 6 The morphology of FMS matrix powders as a function of milling time: **a** 0.5 h, **b** 1 h, **c** 1.5 h, **d** 2 h and **e** 2.5 h

The final stage is the densification via the hot pressing. One of the major advantages of flake powder metallurgy is the high densification possible due to the high ductility of the flake powders.

The variation in flake morphologies for the CMS (coarse matrix size), MMS (medium matrix size) and FMS groups (fine matrix size) as a function of the milling time (0.5, 1, 1.5, 2 and 2.5 h) is shown in Figs. 4, 5 and 6. The milled

powders were found to include undeformed (non flake-like) powders (Figs. 4a, 5a, 6a) after 0.5 h of milling. Therefore, the powder morphology obtained after 0.5 h of milling was not suitable for flake powder metallurgy as a result of the non-homogeneous powder morphology. The initial particle morphology (which was observed to be irregular) transformed to a flake powder morphology after 1 h of milling. The SEM images show that the powder milled for 1 h exhibits a flake morphology (Figs 4b, 5b, 6b). As seen in Figs 4c, d, 5c, d, and 6c, d, the morphologies obtained after 1.5 and 2 h of milling exhibit particle deformation and a homogeneous flake morphology. It is noted that the some milled powders may fracture during particle deformation as a result of ball–powder–ball and ball–powder–vial collisions. However, it is also noted that the deformation process is more dominant than the fracture process due to the relatively ductile nature of the matrix powder. The homogenous flake particle morphology is observed to transform to a non-homogenous flake particle morphology after 2.5 h of milling, as shown in Figs. 4e, 5e and 6e. Therefore, fracture based processes dominate after 2 h of milling, a fact that has been observed by other researchers [21,22]. From the morphological examinations, the flake powders produced using 1, 1.5, and 2 h of milling were observed to comply with the requirements for basic flake powder metallurgy, permitting these flake powders to be used in consolidation or nanocomposite production processes. The effect of the initial particle size of the Al2024 powders on the flake morphology is also explained in Figs. 4, 5 and 6. It is noted that the homogeneous flake morphology decreased with the initial particle size, which is attributed to the ductility of the as-received powders. Finer metal powder is more difficult to solidify than coarse metal powder because finer metal powder solidifies faster and yields a harder product than coarse metal powder during the atomization process. Therefore, the balance between deformation and fracture must be maintained during ball milling of fine ductile powder. Some particles were easily fractured and non-homogeneous flake morphology was observed. However, it is noted that the flake morphology was the dominant mechanism for all the powder groups milled for 1, 1.5 and 2 h.

3.2 Flake Particle Size

In the flake powder metallurgy method, the use of homogeneous flake particles is a key factor to obtaining composites possessing superior physical and mechanical properties. Figure 7 shows the variation in the average particle size as the milling time increases for all matrix groups. The reduction in the particle size of the Al2024 matrix powder is faster in the initial milling stage (0.5 and 1 h). This may be attributed to the initial matrix powder having irregular or ligament-like shapes. These powders are easily deformed by ball collisions and are easily fractured in their weak regions. It is noted that

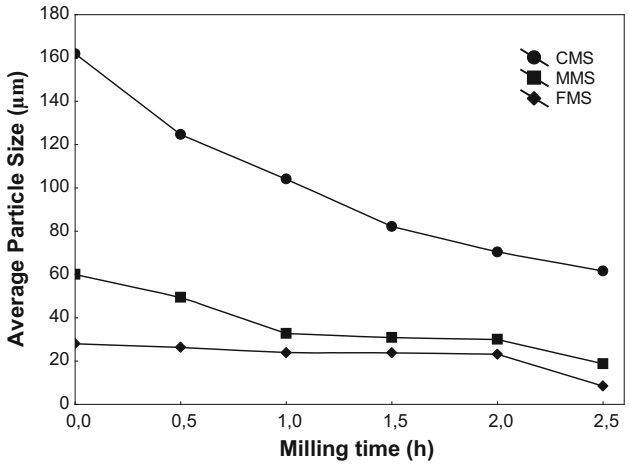

Fig. 7 The change in the average particle size with increasing milling time

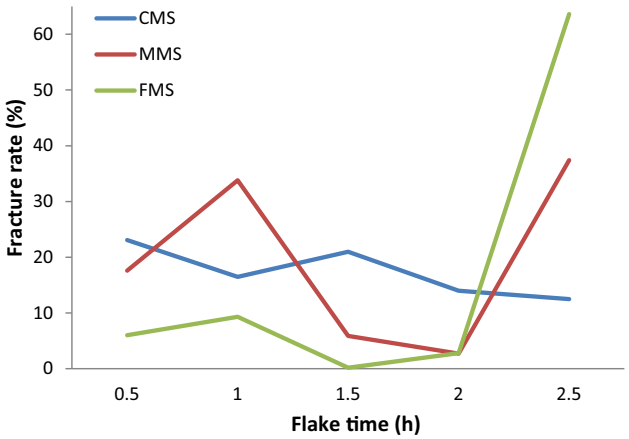

Fig. 8 The change in the fracture rate (%) with increasing milling time for the different matrix groups

the initial powder morphology is an important factor that affects the final particle size [23]. As seen in Fig. 7, the particle size decreases slightly after 1 h of milling because there are no weak regions in the Al2024 powders after this stage. In particular, there was a remarkable decrease in the particle size of the MMS and FMS matrix groups compared to the CMS group. The decrease in the particle size may result from both an increase in the milling time and an increase in the amount of plastic deformation. The average particle size of the CMS matrix powders after 0.5 h of milling was approximately 124 µm, which decreased to 62 µm when the as milling time was increased to 2.5 h. However, the particle size of FMS matrix powders after 0.5 h of milling was approximately 26 µm, which decresaed to 8 µm when the milling time was increased to 2.5 h.

As shown in Fig. 8, the fracture rate (%) or deformation rate (%) can be examined to gain a better understanding of these processes. Fracture rate shows the percentage of the

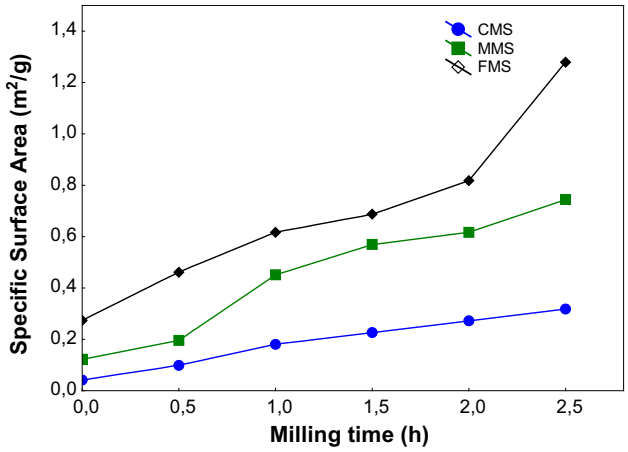

Fig. 9 The change in the specific surface area with increasing milling time

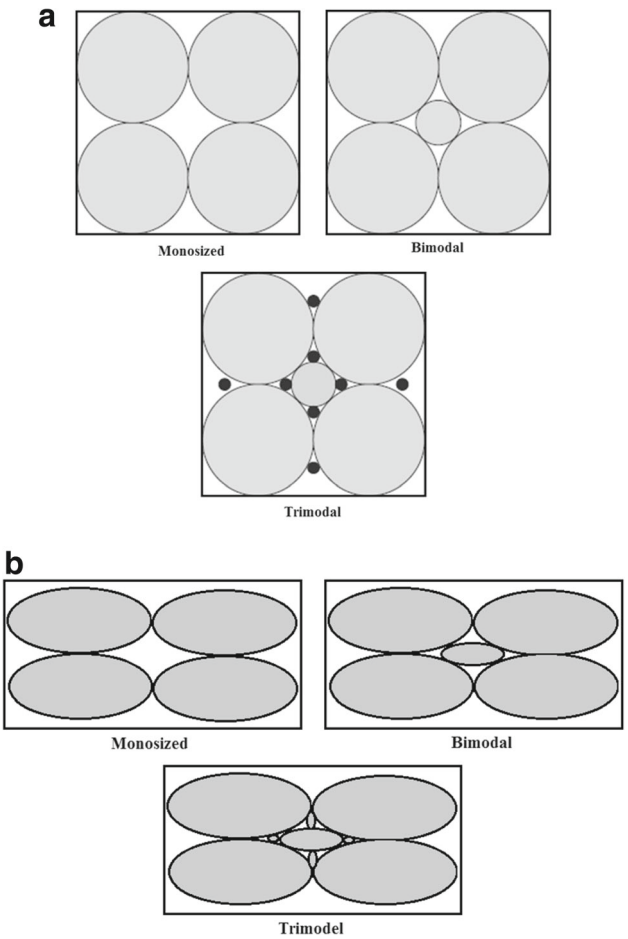

Fig. 10 Particle arrangement for the different particle size distributions: **a** spherical powder and, **b** flake powders

amount of fracture particles in the total powder mass. On the other hand, deformation rate refers to the percentage of the amount of deformed particles in the total powder mass. A

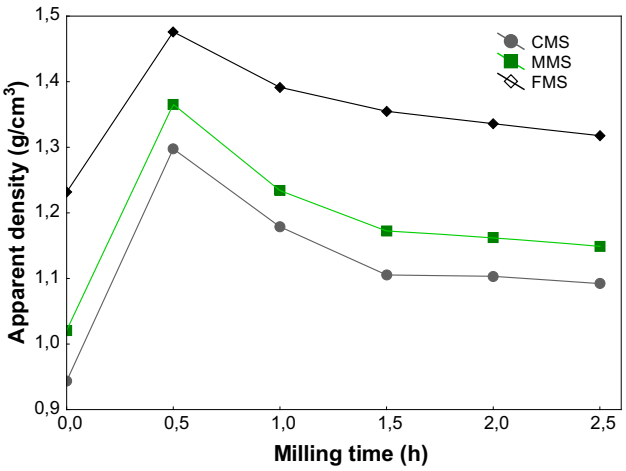

Fig. 11 Effect of milling time on the apparent density of the flake matrix powders

new set of formulas named as the Temel equations were used to calculate the fracture rate (%) or deformation rate [24].

3.3 Specific Surface Area

Specific surface area is a property of metal particles explained as the total surface area of a powder particle per unit of powder mass (m^2/g). As seen in Fig. 9, the specific surface area increased with the ball milling time. The increasing trend for specific surface area with the milling time may be attributed to the fracture processes that occur as a result of the deformation during the ball milling process. It should be noted that the specific surface area increased with decreasing initial particle size of Al2024 alloy powders (Fig. 9). This may be attributed to the fine initial particle size and rapid reduction in the particle size of the FMS matrix powders.

3.4 Apparent Density of the Flake Matrix Powders

Figure 10 shows the particle contacts and arrangement for spherical and flake morphologies, respectively. The packing factor of spherical particles leads to a higher density than other shapes. The packing density decreases as the surface roughness or shape irregularity increases. For a coarse spherical powder, the packing fraction for a loose packing is usually near 60 % of the theoretical value. A higher relative apparent density may be achieved by mixing different sized powders, as shown in Fig. 10. This principle involves using finer particles to fill the voids formed by the larger powders. It is noted that there are a great number of voids within the compacted samples fabricated using flake powders than those fabricated using spherical powders. Therefore, if powder mass includes bimodal or trimodal distributions, the fine powders easily fill the voids and high-density parts can be fabricated. It is noted that metal powders with a very fine particle size provide only

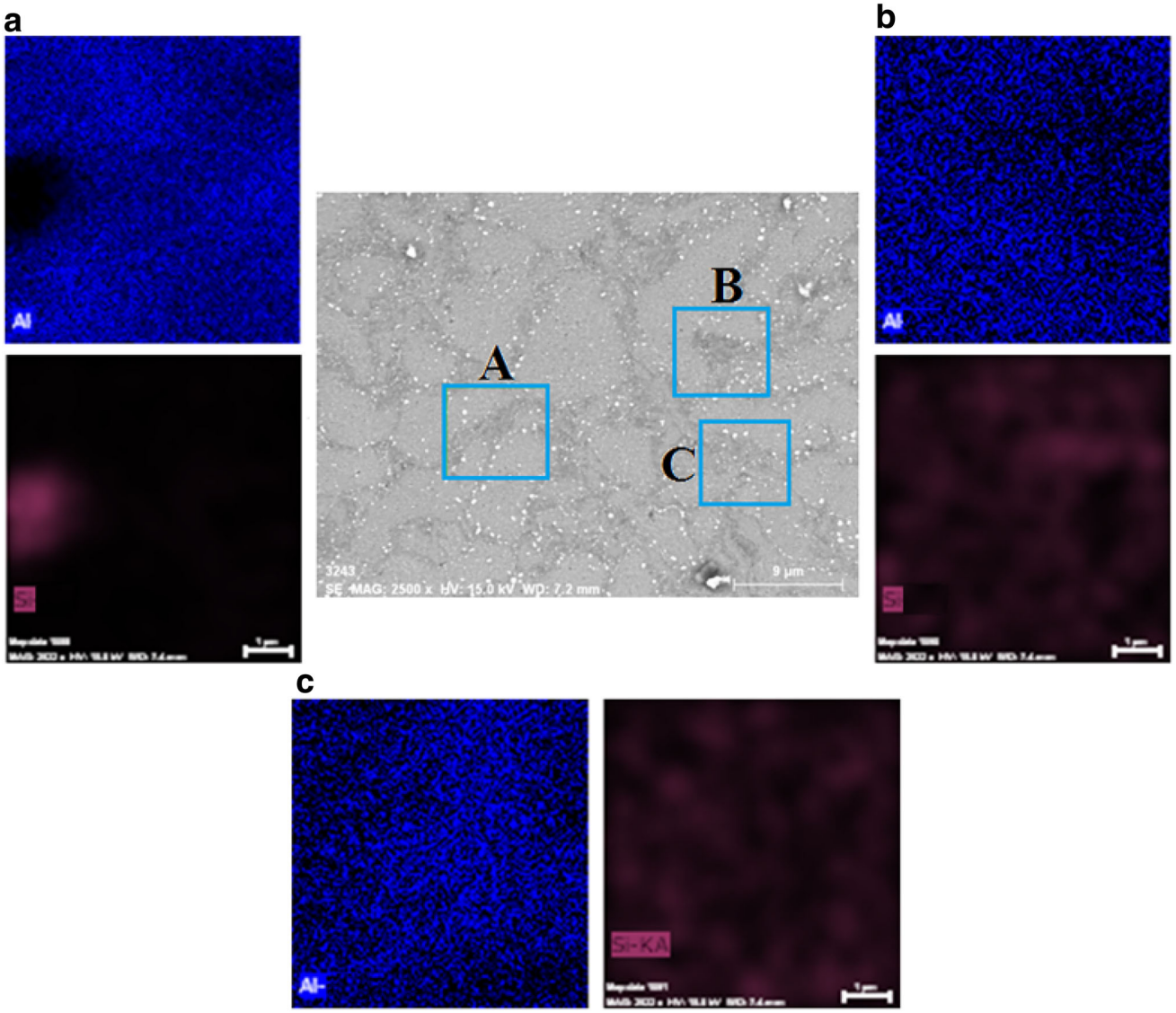

Fig. 12 SEM image and elemental mapping showing the effect of the nanoSiC content on the microstructure and dispersion of the particles in the CMS nanocomposites reinforced with 1 wt% SiC

a small improvement to the apparent density because they easily agglomerate [25,26].

The apparent density increased for all the matrix groups after 0.5 h of milling and then decreased as the ball milling time increased, as shown in Fig. 11. The change in the apparent density is closely related to the powder morphology. The powders are deformed due to high energy collisions with the balls and fractured in their fine regions during the initial stage of mechanical milling. The broken and undeformed powders fill the space formed by the flake powders so that the apparent density increases. The irregular or initial morphology changes to a flake morphology after 1 h of milling and the apparent density decreases as a result of the morphological transformation. It is noted that the flake morphology results in poorer powder packing and a decrease in the apparent density, as shown in Fig. 11.

3.5 Microstructure

The microstructural changes in the nanoSiC particle-reinforced Al2024 alloy matrix composites fabricated using the flake powder metallurgy method are shown in Figs. 12, 13 and 14. The microstructure of the Al2024/SiC nanocomposites consist of a flake-like microstructure with dispersed nanoSiC particles between the Al2024 matrix powders with grain boundaries containing the reinforcement particles. The EDS mapping of the SiC (shown in purple) in Figs. 12, 13 and 14 shows that the SiC nanoparticles are dispersed

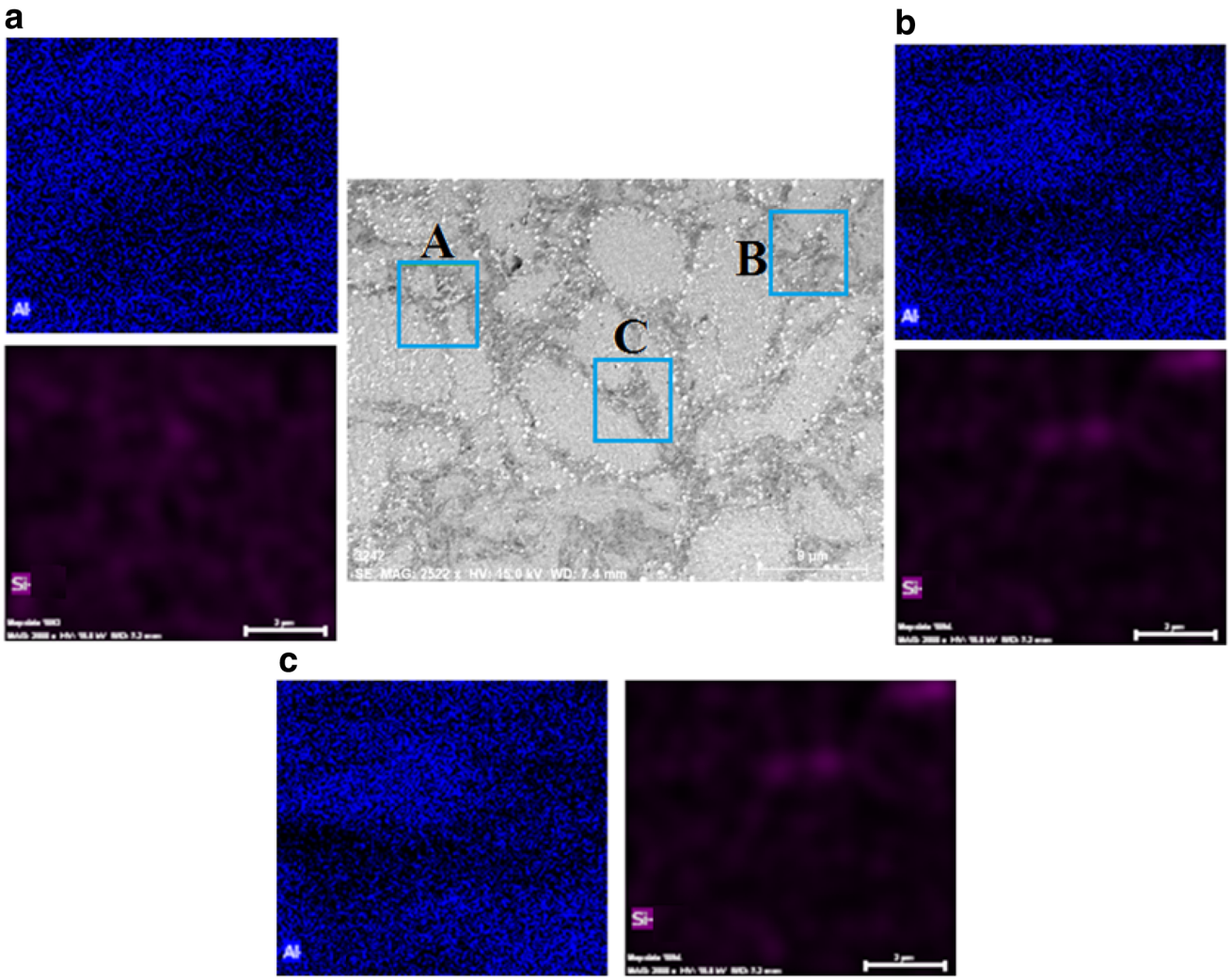

Fig. 13 SEM image and elemental mapping showing the effect of the nanoSiC content on the microstructure and dispersion of the particles in the CMS nanocomposites reinforced with 3 wt% SiC

at the grain boundaries. The nanoSiC content in the grain boundaries increased with the overall nanoSiC particle content. In other words, higher amounts of nanoSiC particles in the grain boundaries of the nanocomposites were observed. The distribution of nanoparticles in the 1 wt% SiC and 3 wt% SiC-reinforced nanocomposites was homogenous compared to the 5 wt% SiC-reinforced nanocomposites. This is attributed to increasing number of nanoparticles in the composite mixture. Moreover, the agglomeration content of the SiC nanoparticles increased due to the increase in the nanoparticle content, as shown in Figs. 12, 13 and 14. Another important microstructural observation was the increase in the porosity content for the nanocomposites reinforced 5 wt%. The higher porosity content is mainly due to the lower consolidation capability (compressibility) of the mixture when this amount of nanoSiC particles is used.

3.6 Density and Hardness

The effect of the SiC content and Al2024 matrix size on the hot pressed density is shown in Fig. 15. This figure showed that the hot pressed density decreased with increases in the nanoSiC content. The reason for this was the reduction in the pressing capacity of the nanocomposites as the nanoSiC content increased. This was due to the higher hardness of SiC particles. Another reason for this reduction was the inhibitive effect of the nanoSiC particles on the sintering process. The particles a pure Al2024 alloy matrix as a result the higher melting temperature of the SiC (2730 °C), which leads to a weak network. Figure 15 shows that the hot pressed density decreased as the milling time increased. The reason for this is that when pressure is applied, the high friction present occurred between the Al2024 matrix powders due their flake morphology reduced their densi-

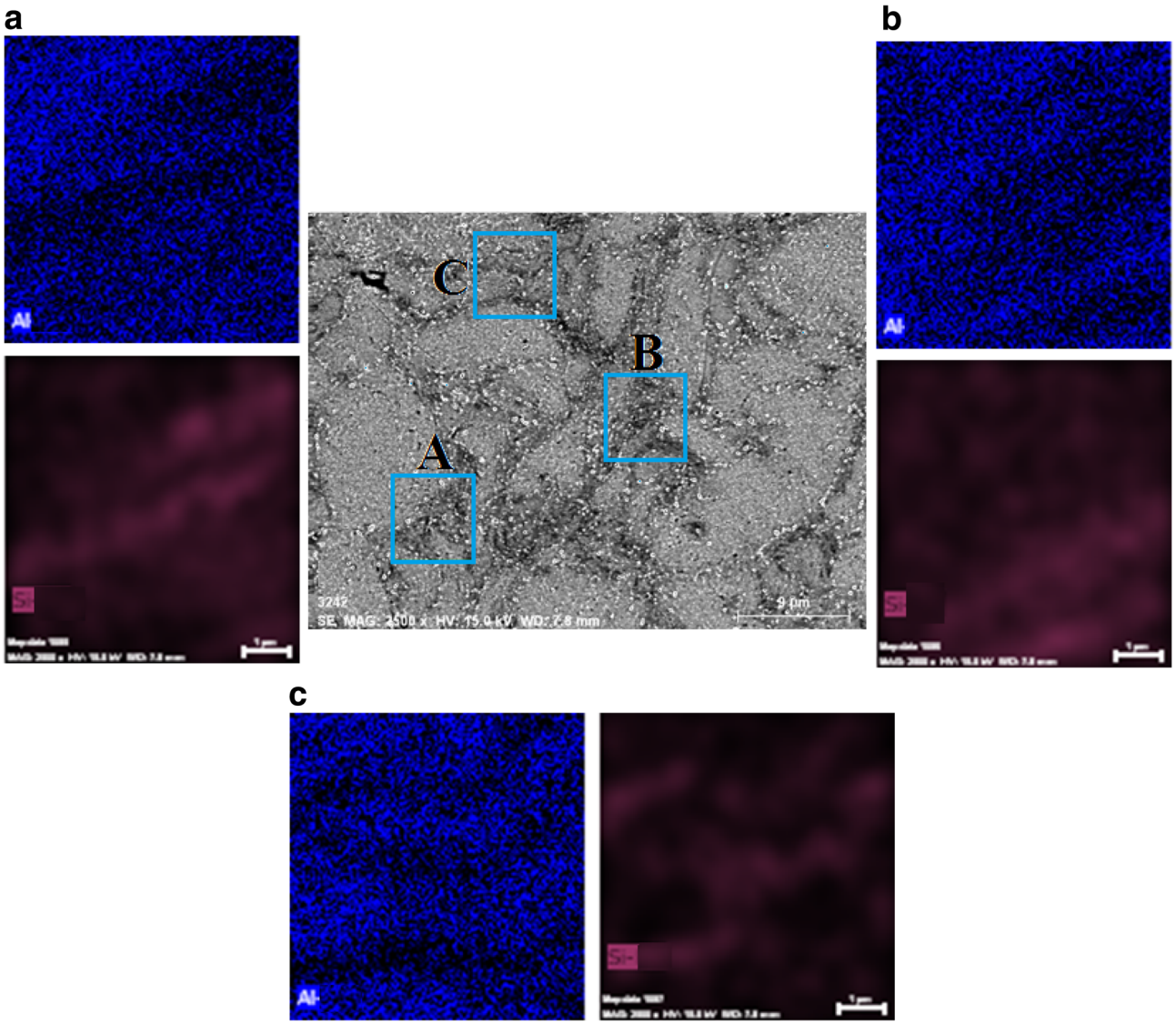

Fig. 14 SEM image and elemental mapping showing the effect of the nanoSiC content on the microstructure and dispersion of the particles in the CMS nanocomposites reinforced with 5 wt% SiC

fication capability, eventually leading to a decrease in the density value. This may also be attributed to the relationship between the milling time and the ductility of the milled powders. It was observed that the ductility of the flake powders decreased as the milling time increased. However, decreasing the size of the Al2024 matrix powders increased the density of the Al2024/SiC nanocomposites by minimizing the friction between the fine flake particles (Fig. 15). The agglomeration content of the coarse flake particles is greater than that for the fine flake particles. Therefore, the consolidation ability of the Al2024/SiC nanocomposites increased as the particle size of the Al2024 matrix powders decreased.

The results of the Brinell hardness measurements from the Al2024/SiC nanocomposites fabricated using the different ball milling times, SiC contents and matrix sizes are presented in Fig. 16. The hardness of the hot pressed Al2024/SiC nanocomposites exhibited an increase as the amount of SiC particles increased. The increase in the hardness as the SiC content increased resulted from increase of nanoSiC particle content within the grain boundaries, which was observed in the SEM images. It is noted that the number of nanosized particles is significantly higher than the number of microsized particles for the same amount of SiC particles (based on the wt%). As seen in Fig. 16, the hardness of the Al2024/SiC nanocomposites increased with increasing the milling time for all compositions. The main reason for this may attributed to a better distribution of the SiC nanoparticles within the Al2024 matrix. Moreover, this increase may be attributed to work hard-

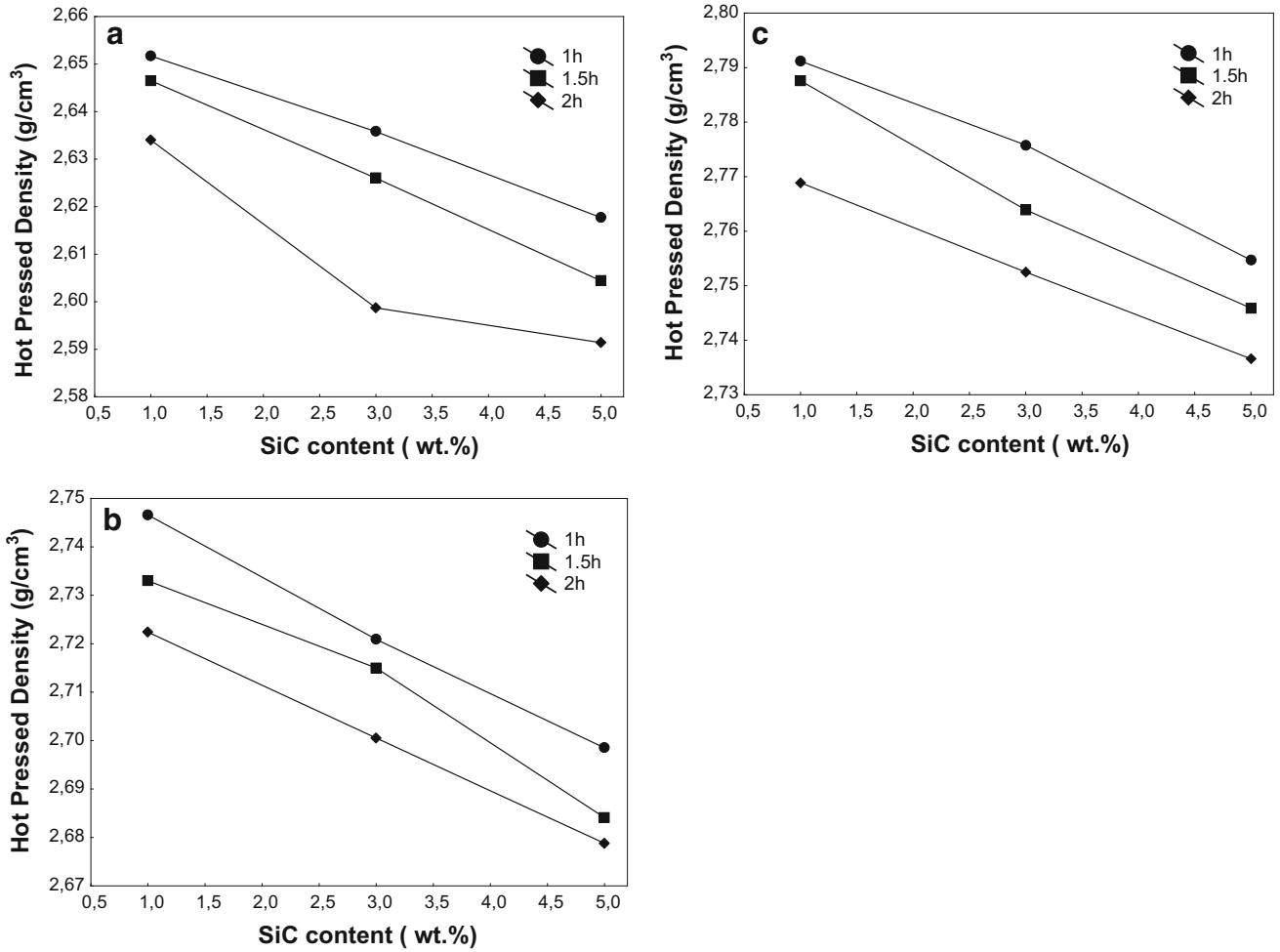

Fig. 15 The change in the pressed density with increasing nanoSiC content and ball milling time: **a** CMS group, **b** MMS group and, **c** FMS group

ening that occurred during ball milling. The hardness of the Al2024/SiC nanocomposites synthesized from the FMS matrix powders was significantly higher than that of the Al2024/SiC nanocomposites synthesized using the CMS matrix powders. This increase in hardness may be attributed to a more homogeneous distribution of the nanoSiC particles within the Al2024 alloy matrix. The distance between the nanoparticles decreased with the matrix size. This caused an increase in the number of nanoparticles within a specific area, leading to the observed hardness increase (Fig. 16a–c).

4 Conclusions

The milled powders obtained after 0.5 h of milling contain some unflaked powder due to a smaller amount of deformation. However, the critical deformation ratio was exceeded after 2 h of milling, causing fracture processes to dominate over deformation processes. Therefore, the milled powders obtained after 0.5 and 2.5 h of milling were not used during the consolidation stage. The particle size of the CMS matrix powder after 0.5 h of milling was approximately 124 μm, which decreased to 62 μm as milling time increased to 2.5 h. However, the particle size of the FMS matrix powder after 0.5 h of milling was approximately 26 μm, which decreased to 8 μm as milling time increased to 2.5 h. The apparent density of the flake Al2024 matrix powders increased after the initial ball milling stage and decreased as the milling time increased due to changes in the arrangement of the particles and changes in the amount of voids within the powder. For CMS, MMS and FMS matrix powders synthesized by 1.5 h of milling, with increasing the nanoSiC particle content from 1 to 5 (wt%), the hot pressing density decreases from 2.62 to 2.57 g/cm^3, from 2.72 to 2.70 g/cm^3 and from 2.79 to 2.75 g/cm^3, respectively. The hardness of the Al2024/SiC nanocomposites increased as the SiC content and the size of Al2024 matrix powders

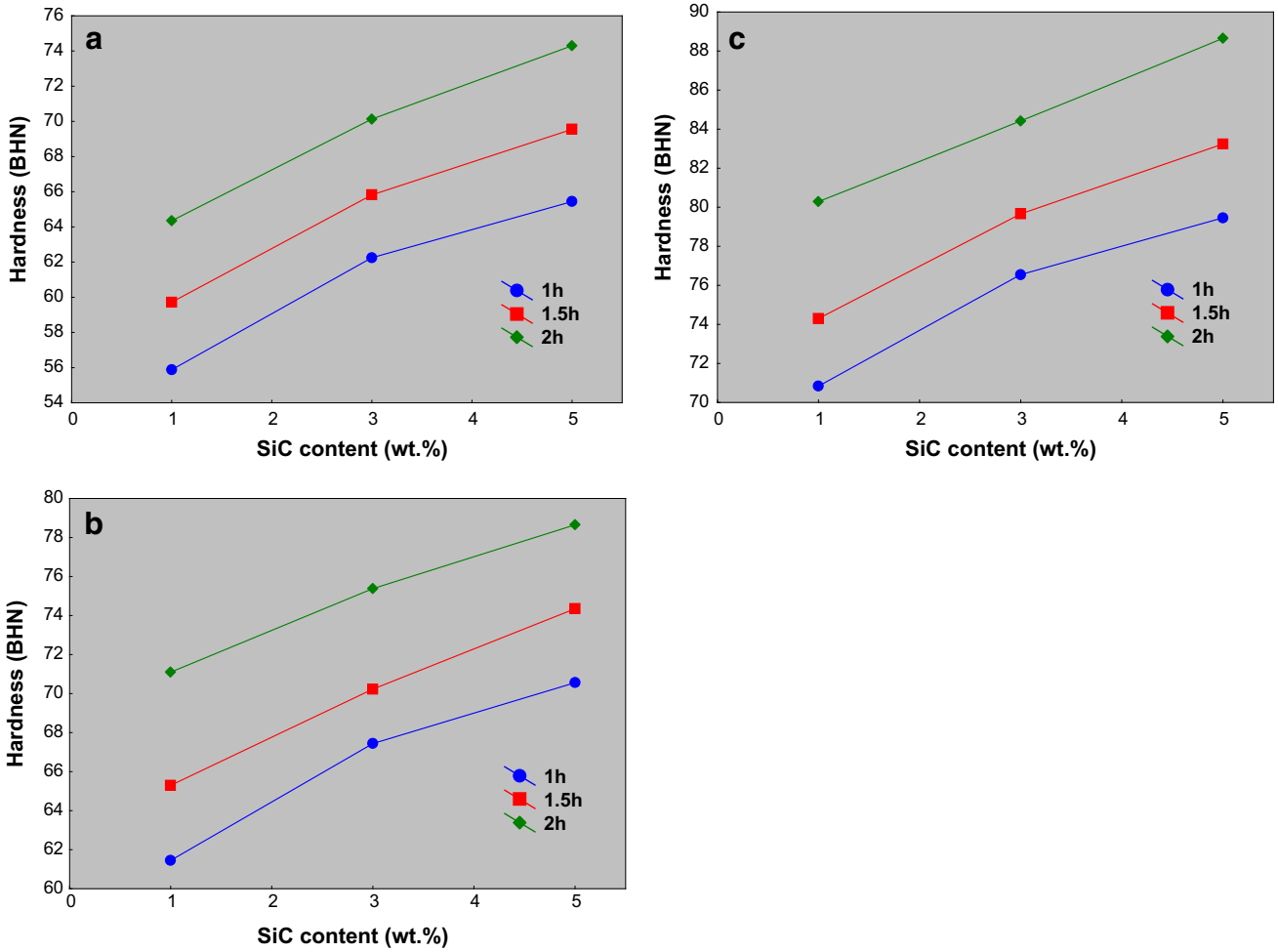

Fig. 16 Dependence of hardness of Al2024-SiC nanocomposites on different nanoSiC content and different ball milling time: **a** CMS group, **b** MMS group and, **c** FMS group

increased. The maximum hardness value of 88.65 Brinell are obtained for Al2024-5 wt% SiC nanocomposites fabricated by FMS matrix powders synthesized by 2 h of milling.

References

1. Topcu, I.; Gulsoy, H.O.; Kadioglu, N.; Gulluoglu, A.N.: Processing and mechanical properties of B_4C reinforced Al matrix composites. J. Alloys Compd. **482**, 516–521 (2009)
2. Ozden, S.; Ekici, R.; Nair, F.: Investigation of impact behavior of aluminum based SiC particle reinforced metal-matrix composites. Compos. Part A **38**, 484–494 (2007)
3. El-Kady, O.; Fathy, A.: Effect of SiC particle size on the physical and mechanical properties of extruded Al matrix nanocomposites. Mater. Des. **54**, 348–353 (2014)
4. Canakci, A.; Varol, T.: Microstructure and properties of AA7075/Al-SiC composites fabricated using powder metallurgy and hot pressing. Powder Technol. **268**, 72–79 (2014)
5. Canakci, A.; Ozsahin, S.; Varol, T.: Prediction of effect of reinforcement size and volume fraction on the abrasive wear behavior of AA2014/B4Cp MMCs using artificial neural network. Arab. J. Sci. Eng. **8**, 6351–6361 (2014)
6. Shabestari, S.G.; Ghoncheh, M.H.; Momeni, H.: Evaluation of formation of intermetallic compounds in Al2024 alloy using thermal analysis technique. Thermochim. Acta **589**, 174–182 (2014)
7. Kök, M.: Abrasive wear of Al_2O_3 particle reinforced 2024 aluminum alloy composites fabricated by vortex method. Compos. Part A **37**, 457–464 (2006)
8. Suryanarayana, C.; Al-Aqeeli, N.: Mechanically alloyed nanocomposites. Prog. Mater. Sci. **58**, 383–502 (2013)
9. Izadi, H.; Nolting, A.; Munro, C.; et al.: Friction stir processing of Al/SiC composites fabricated by powder metallurgy. Prog. Mater. Sci. **213**, 1900–1907 (2013)
10. Cavdar, U.; Atik, E.; Akgul, M.B.: Magnetic-thermal analysis and rapid consolidation of Fe-3 wt% Cu powder metal compacts sintered by medium-frequency induction-heated system. Powder Metall. Met. Ceram. **53**, 191–198 (2014)
11. Umasankar, V.; Xavior, M.A.; Karthikeyan, S.: Experimental evaluation of the influence of processing parameters on the mechanical properties of SiC particle reinforced AA6061 aluminum alloy matrix composite by powder processing. J. Alloys Compd. **582**, 380–386 (2014)

12. Varol, T.; Canakci, A.: Synthesis and characterization of nanocrystalline Al2024-B_4C composite powders by mechanical alloying. Philos. Mag. Lett. **93**, 339–345 (2013)
13. Canakci, A.; Varol, T.; Cuvalci, H.; Erdemir, F.; Ozkaya, S.; Yalcin, E.D.: Synthesis of novel CuSn10-graphite nanocomposite powders by mechanical alloying. Micro Nano Lett. **9**, 109–112 (2014)
14. Jiang, L.; Li, Z.; Fan, G.; et al.: The use of flake powder metallurgy to produce carbon nanotube (CNT)/aluminum composites with a homogenous CNT distribution. Carbon **50**, 1993–1998 (2012)
15. Kai, X.; Li, Z.; Fan, G.; et al.: Strong and ductile particulate reinforced ultrafine-grained metallic composites fabricated by flake powder metallurgy. Scr. Mater. **68**, 555–558 (2013)
16. Zhang, W.; Li, Z.; L. Jiang, L.; et al.: Flake thickness effect of Al_2O_3/Al biomimetic nanolaminated composites fabricated by flake powder metallurgy. Mater. Sci. Eng. A **594**, 324–329 (2014)
17. Canakci, A.; Varol, T.; Nazik, C.: Effects of amount of methanol on characteristics of mechanically alloyed Al-Al_2O_3 composite powders. Mater. Technol. **27**, 320–327 (2012)
18. Canakci, A.; Varol, T.; Ozsahin, S.: Prediction of effect of volume fraction, compact pressure and milling time on properties of Al-Al_2O_3 MMCs using neural networks. Met. Mater. Int. **19**, 519–526 (2013)
19. Fogagnolo, J.B.; Ruiz-Navas, E.M.; Robert, M.H.; Torralba, J.M.: The effects of mechanical alloying on the compressibility of aluminum matrix composite powder. Mater. Sci. Eng. A **355**, 50–55 (2003)
20. Hesabi, Z.R.; Hafizpour, H.R.; Simchi, A.: An investigation on the compressibility of aluminum/nano-alumina composite powder prepared by blending and mechanical milling. Mater. Sci. Eng. A **454–455**, 89–98 (2007)
21. Shukla, A.K.; Narayana, S.V.S.; Murty, R.; et al.: Effect of powder milling on mechanical properties of hot-pressed and hot-rolled Cu–Cr–Nb alloy. J. Alloys Compd. **580**, 427–434 (2013)
22. Madavali, B.; Lee, J.H.; Lee, J.K.; et al.: Effects of atmosphere and milling time on the coarsening of copper powders during mechanical milling. Powder Technol. **256**, 251–256 (2014)
23. Canakci, A.; Varol, T.; Ertok, S.: The effect of mechanical alloying on Al_2O_3 distribution and properties of Al_2O_3 particle reinforced Al-MMCs. Sci. Eng. Compos. Mater. **19**, 227–235 (2012)
24. Canakci, A., Varol, T., Erdemir, F.: The effect of flake powder metallurgy on the microstructure and densification behavior of B_4C nanoparticle-reinforced Al–Cu–Mg alloy matrix nanocomposites. Arab. J. Sci. Eng. doi:10.1007/s13369-015-1969-2
25. German, R.M.: Particle Packing Characteristics. Metal Powder Industries Federation, New Jersey (1999)
26. Smith, L.N.; Midha, P.S.: Computer simulation of morphology and packing behaviour of irregular particles, for predicting apparent powder densities. Comput. Mater. Sci. **7**, 377–383 (1997)